Polarization investigation of a tunable high-speed short-wavelength bulk-micromachined MEMS-VCSEL

(article starts on next page)

Polarization Investigation of a Tunable High-Speed Short-Wavelength Bulk-Micromachined MEMS-VCSEL

H. A. Davani[a], B. Kögel [b], P. Debernardi [c], C. Grasse [d], C. Gierl [a], K. Zogal [a], Å. Haglund [b], J. Gustavsson [b], P. Westbergh [b], T. Gründl [d], P. Komissinskiy [a], T. Bitsch [a], L. Alff [a], F. Küppers [a], A. Larsson [b], M.-C. Amann[d], P. Meissner[a]

[a]Technical University Darmstadt, Merkstr. 25/Petersenstr. 23, Darmstadt, Germany
[b] Chalmers University of Technology, Gothenburg, Sweden
[c] Instituto di Elettronica e di Ingegneria dell'Informazione e delle Telecomunicazioni, Corso Duca degli Abruzzi 24,Torino,Italy
[d]Walter Schottky Institute,Am Coulombwall 3,Garching, Germany

ABSTRACT

We report the investigation of the state of polarization (SOP) of a tunable vertical-cavity surface-emitting laser (VCSEL) operating near 850 nm with a mode-hop free single-mode tuning range of about 12 nm and an amplitude modulation bandwidth of about 5 GHz. In addition, the effect of a sub-wavelength grating on the device and its influence on the polarization stability and polarization switching has been investigated. The VCSEL with an integrated sub-wavelength grating shows a stable SOP with a polarization mode suppression ratio (PMSR) more than 35 dB during the tuning.

Keywords: Tunable laser, VCSEL, Tunable VCSEL, Polarization, sub-wavelength grating

1. INTRODUCTION

High-speed tunable short-wavelength VCSELs are suitable for parallel optical interconnects with applications in massively parallel processing systems.[1] In this application a single array of tunable VCSELs can replace a multiple array of fixed-wavelength VCSELs. These VCSELs can be used also in reconfigurable multiprocessor interconnects in combination with selective optical broadcast components (SOB).[2] By changing the wavelength of the tunable VCSEL one processor node on the transmitter side can address different processors on the receiver side. These VCSELs have to provide a stable and reproducible tuning, a stable state of polarization and high bit rate operation.

Due to the relative large transverse extend in combination with a symmetric geometry and isotropic material properties, the VCSEL tends to lase in several transverse modes with an unpredictable state of polarization. These linear states of polarization lie in the plane of the epitaxial layers and they are normally polarized in (011)- or $(0\bar{1}1)$-crystallographic direction. However, the polarization often randomly switches between these two directions because of temperature, injection current and optical feed-back effects.[3] The high-speed modulation has also effect on polarization and can make it unstable.[4] In case of tunable VCSELs, the polarization may also switch during the tuning of the VCSEL.

There are several techniques to suppress the higher order transverse modes in VCSELs. Some of them are using an oxide aperture, extended cavity technique, introducing two-dimensional photonic crystal in the VCSEL, introducing shallow surface relief in the top mirror and using a buried tunnel junction. All these techniques have their advantages and disadvantages.[5] In the device presented here, a half-symmetric resonator, achieved by a curved membrane, in combination with an oxide aperture supports the fundamental mode (Gaussian beam) of the VCSEL and makes the single transversal mode operation of the device possible. This plane concave resonator makes it possible to fit the beam waist of the fundamental mode (by changing the air-gap and the radius of curvature (RoC)) into the oxide aperture and thus be able to use an larger oxide aperture. Larger

Further author information: (Send correspondence to Hooman A. Davani)
Hooman A. Davani: E-mail: Davani@ont.tu-darmstadt, Telephone: +49 6151 166848

Vertical-Cavity Surface-Emitting Lasers XVI, edited by Chun Lei, Kent D. Choquette, Proc. of SPIE Vol. 8276, 82760T · © 2012 SPIE · CCC code: 0277-786X/12/$18 · doi: 10.1117/12.908262

oxide aperture increases the gain of the device during the single-mode operation.[6] The limitation for single-mode operation is then the nonhomogeneous current distribution in the half-VCSEL. If the current density is much higher at the edges compared to the center of the device then the next transverse modes will get a higher gain and start to lase. With this method we have achieved a transversal side-mode suppression ratio (SMSR) higher than 30 dB.

To be able to control the state of polarization, the introduced anisotropy must of course be stronger than the inherent anisotropy of the device.[5] For non-tunable VCSELs some polarization controllling techniques have been reported. For example, gain anisotropy is achieved by epitaxial growth on non-(100) substrate such as GaAs (311)A[7] and GaAs (311)B.[8] The drawback of using non-(100) substrates is that it becomes more difficult to fabricate a symmetric oxide aperture. Other polarization stabilizing techniques are using an asymmetric current injection to introduce both anisotropic gain and cavity losses,[9] introducing anisotropic strain in the VCSEL via etching deep trenches close to the VCSEL aperture along the preferential polarization direction[10] or via using strained T-bars[11] and implementing a surface grating.[5] All these methods have their drawbacks and advantages discussed partly in.[5] In this paper we have used a sub-wavelength grating on the half-VCSEL air interface to select one polarization mode. A PMSR of about 35 dB has been achieved with this technique.

2. DESIGN AND FABRICATION

2.1 Half-VCSEL

The half-VCSEL part of the device is a tunable VCSEL without the top mirror membrane. It consists of an undoped GaAs substrate, a n-type GaAs contact layer above the n-contact (Ni/Ge/Au), an n-doped DBR with alternating pairs of $Al_{15}GaAs/Al_{85}GaAs$ (with a total reflectivity of $> 99.9\%$), a gain region with 3 GaAs quantum wells (QWs) and a top p-region as can be seen in the Fig. 1a. The p-doped region contains three 50

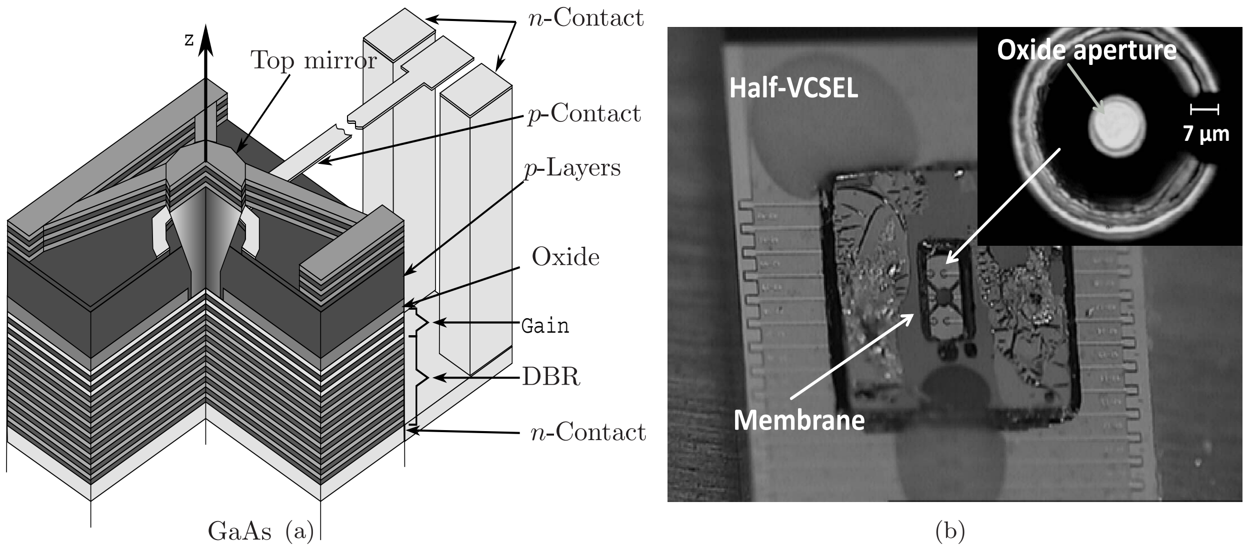

Figure 1. (a) Cross-section view of the tunable VCSEL. (b) Microscope images of the whole device and infra-red microscope image of one half-VCSEL on the chip.

nm thick p^+-doped layers for current spreading below the top p-contact layer and an oxide aperture for lateral current confinement just above the gain region. The current aperture also defines simultaneously the gain area and acts for the optical confinement. To avoid index guiding, the oxide aperture is positioned at a node of the longitudinal optical field. The oxide aperture layer is an aluminum rich AlGaAs layer which is selectively oxidized.[5] The half-VCSEL has a non-resonant design[12] where the optical field has its minimum (node) at the semiconductor-air interface. Additionally the semiconductor-air interface can be covered with a $\lambda/4$-thick SiN_x-coating to increase the nominal reflectivity from the interface and thus reduce the required threshold gain.

The half-VCSEL has a mesa diameter of about 40 μm and an oxide aperture of about 11 μm (Fig. 1b). To be able to connect the VCSEL to high frequency probes outside the support frame of the micromachined movable mirror, a 1.3 mm long microstrip line connects the VCSEL to ground-signal-ground (G-S-G) pads (Fig. 1a). The n-contact layer acts as a ground plane for the transmission line. A 6 μm thick layer of the dielectric material benzocyclobutene (BCB) with a low dielectric constant of 2.6, separates the transmission line from the ground plane. An amplitude modulation bandwidth of 5 GHz has been already presented using these devices.[6]

2.2 Membrane

The membrane, which serves as the tunable top mirror (Fig. 1), consists of AlGa(In)As layers grown by molecular beam epitaxy (MBE) on undoped GaAs substrates. The high-index layers have an aluminum-content of 14% percent and the low-index layers, on the other hand, are composed of $Al_{0.85}GaAs$. This results in a refraction index difference of about 0.4. Thus for achieving a 99.8% reflection 22.5 $\lambda/4$-thick pairs are needed. To realize a well-defined curvature of this DBR structure, after removing the substrate, a compressive stress gradient is embedded by adding indium to the first nine high index layers.

Finally, to define an ohmic heat generation in the mirror, the first 17 grown mirror pairs are doped with silicon to achieve a n-doping in the range from $1x10^{18}cm^{-3}$ to $5x10^{17}cm^{-3}$. The reflection measurements show that the grown DBR has a center wavelength of 851 nm and the bandwidth of the mirror defined by a reflectivity of 99.7% is around 40 nm.

The fabrication process of the membrane is mainly based on the contact lithography, wet etching of the front and back side and metalization.[13] The resulting membrane got an air-gap around 3.5 μm and a RoC of about 2.5 mm. These parameters yield a spot size of about 10 μm[6] which is in the same range of half-VCSEL oxide aperture (Sec. 2.1). After processing, the membrane is adjusted and then fixed on top of the half-VCSEL as shown in Fig. 1b. The actuation of the membrane is electro-thermal. A heating current flowing through the membrane suspension beams, thermally expands the beam length and changes the resonant cavity length thus the lasing wavelength.[13]

2.3 Sub-Wavelength Grating

A sub-wavelength grating is a grating which has a periodicity shorter than the optical wavelength in the material.[14] The electrical field of the wave polarized parallel or perpendicular to the sub-wavelength grating experiences the grating as a homogeneous medium, but with different effective refractive indices ($n_\parallel$ for the parallel field and $n_\perp$ for the perpendicular field) given by:[15]

$$n_\parallel^2 = \frac{d_1 n_1^2 + d_2 n_2^2}{d_1 + d_2} \quad ; \quad n_\perp^2 = \frac{(d_1 + d_2) n_1^2 n_2^2}{d_2 n_1^2 + d_1 n_2^2}. \tag{1}$$

Here, d_1 is the width of the ridges, n_1 is the refractive index of the material, d_2 is the width of the grooves and n_2 is the refractive index of the ambient material (i.e. $n_2 = 1$ in case of air) as shown in Fig. 2. The effective

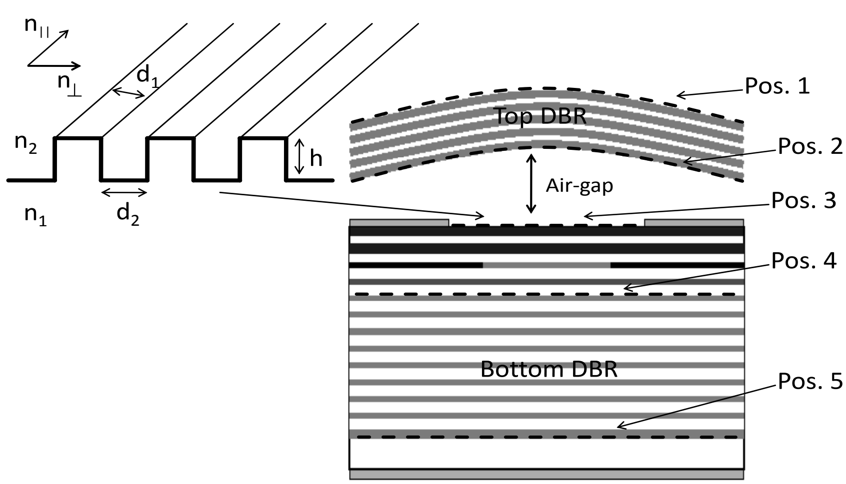

Figure 2. Sub-wavelength Grating pattern and possible positions to implement the grating in the VCSEL.

refractive index is higher in the direction parallel to the grating. The difference is maximum for a duty cycle (defined as ridge width divided by grating period $(d_1 + d_2)$) of around 50%, i.e. $d_1 = d_2$. This can be used to manipulate the reflection phase and adjust the threshold gain (difference) of two polarization modes. Using this simple model, the polarization selectivity can be calculated by means of one-dimensional transfer matrix simulations.

There are several positions to implement the sub-wavelength grating into the device: on the bottom of the bottom mirror, on the top of the bottom mirror, at the half-VCSEL air interface, on the bottom of the top mirror and on the top of the top mirror (Fig. 2). All these positions have different difficulties to be implemented into the device and they have different impact on polarization selectivity too. In the presented device the grating has been implemented on position 3 (Fig. 2). By changing the grating parameters such as duty cycle, etching depth (h in Fig. 2) and grating period, the threshold gain of polarization modes and the threshold gain difference between two polarization modes changes thus the PMSR changes too. Fig. 3 shows the one dimensional simulations for a case with a grating period of 200 nm and different duty cycles and different etching depth. There can be seen that the threshold gain difference between the polarization modes increases for the smaller duty cycles and larger etching depth. Different grating parameter have been implemented on different half-VCSELs of the chip to be able to compare their impact later. The sub-wavelength grating has been implemented on the top

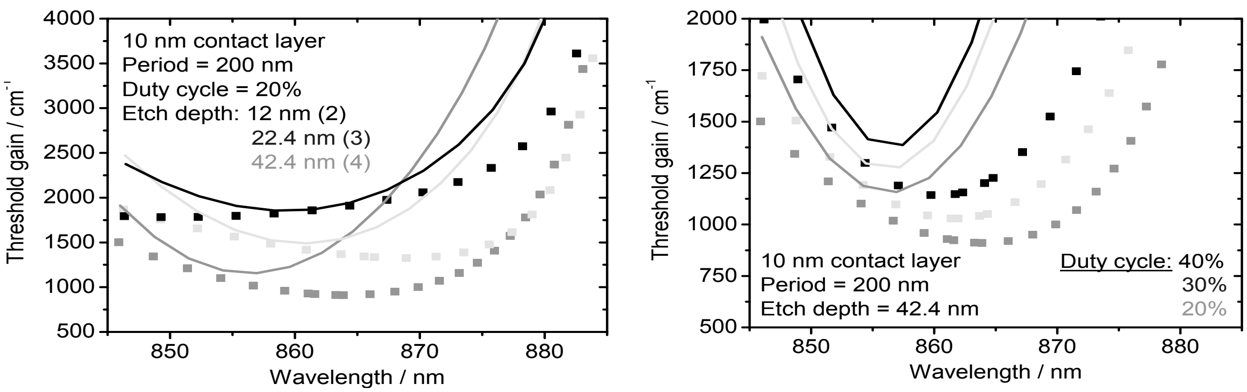

Figure 3. One dimensional simulations for threshold gain over wavelength for a grating period of 200nm and a top p-contact layer of 10 nm. The lines indicate polarization direction parallel to the grating and the dots are the perpendicular one. (a) For different etching depth. (b) For different duty cycles.

of the half-VCSEL in (011) crystallographic direction by means of e-beam lithography and dry-etching. Fig. 4 shows the high resolution electron microscope (HREM) image and atomic force microscope (AFM) image of the grating on the investigated half-VCSEL after finishing the device processing. The images show that finally a period of about 200 nm and an etch depth of $h \approx 50$ nm has been achieved. The irregularity in the grating (Fig. 4) compared to the ideal case from Fig. 2 is because the $\lambda/4$-thick coating (Sec. 2.1) on the grating is deposited later.

3. MEASUREMENTS

3.1 Measurement Setup

Two setups have been used to investigate the device. In the first setup the out coming light from the VCSEL has been coupled directly to a multi-mode fibre and the power and spectrum has been measured in an optical power meter or an optical spectrum analyzer (OSA). In the polarization diversity setup (Fig. 5) the out coming light from the VCSEL is collimated with a collimation lens and is redirected into the first polarization cube (to separate the orthogonal polarizations) via a gold mirror with a very low polarization dependent attenuation. A half-wave plate has been used in front of the cube to fit the polarization axis of the light into the axis of the cube. Due to the low polarization selectivity of the polarization cube in one direction, a second polarization cube in opposite direction has been used in that direction. At the output of the cubes the light has been focused

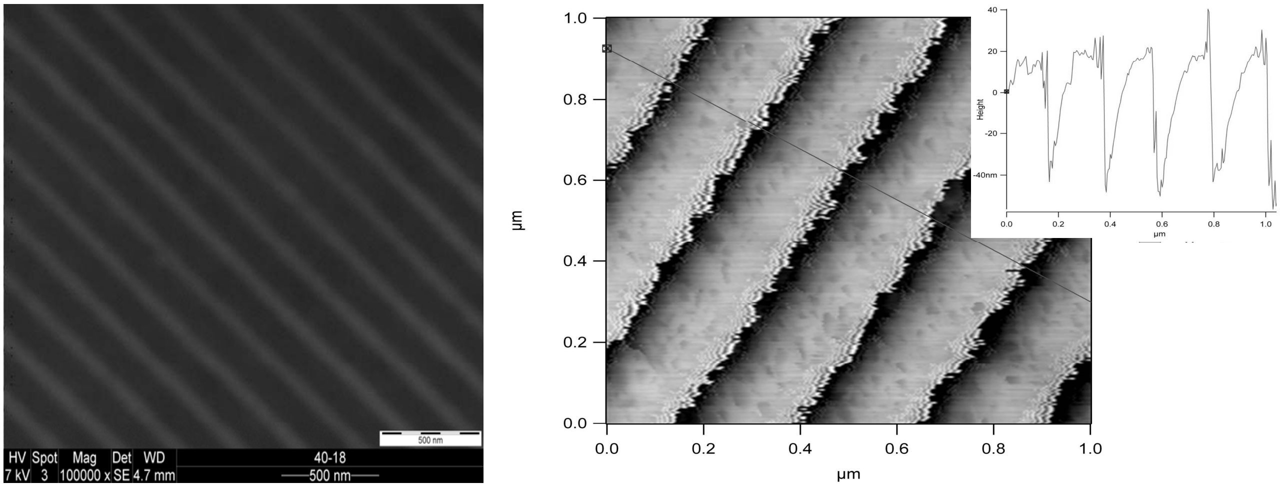

(a) (b)

Figure 4. (a) HREM image and (b) AFM image of the half-VCSEL after deposition of the $\lambda/4$-thick SiN_x-coating.

into the fibers with focusing lenses. A polarization filter is used after the collimation Lens too, to determine the orientation of the polarization compared to the gratings orientation.

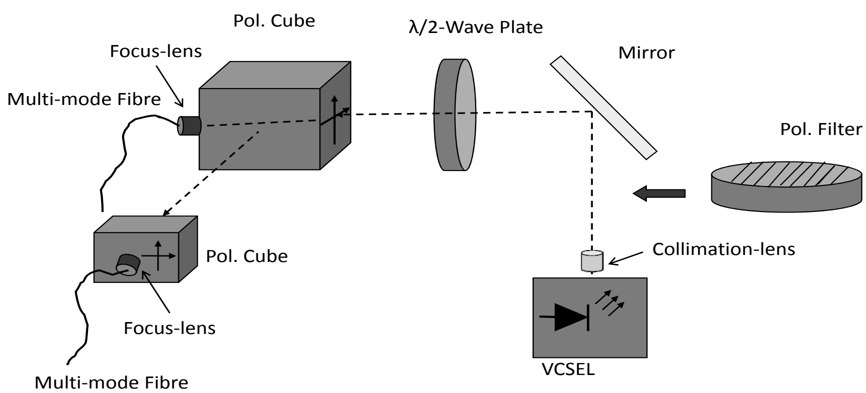

Figure 5. Polarization diversity setup.

3.2 Measurement Results

At first a half-VCSEL without the sub-wavelength grating from the chip (Fig. 1b) has been chosen and the membrane has been adjusted on it. Coupling the light into the fibre without any separation of the states of polarizations, the tuning spectrum over the entire tuning range (by changing the membrane current, Sec. 2.2) for a bias current of 5 mA and has been measured (Fig. 6a). The figure shows the tuning range (the envelope) of about 12 nm (from 827 nm to 839 nm) with a SMSR higher than 30 dB. The maximum output power measured at the wavelength of 830 nm is about 0.08 mW at the thermal rollover current of 5.5 mA with a threshold current of 2.5 mA (Fig. 6b). Using the polarization diversity setup (Fig. 5) the tuning spectrum for each polarization direction has been measured separately as can be seen in Fig. 7. The polarization is unstable at around 827 nm and changes from one to the another one. For the higher wavelength the polarization in (011)-direction is the dominant one and from 833 nm the dominant polarization direction switches in $(0\bar{1}1)$-direction.
The same experiments with the same membrane has been then repeated on the other devices with grating from that chip as shown in Fig. 8. The half-VCSELs are on the same chip and are the same as the previous experiment but the only different is that they have additionally the sub-wavelength grating. The fiber coupled tuning range (Fig. 8a) is about 11 nm from 834 nm to 844 nm for a constant laser bias of 5 mA. A PMSR of larger than 35

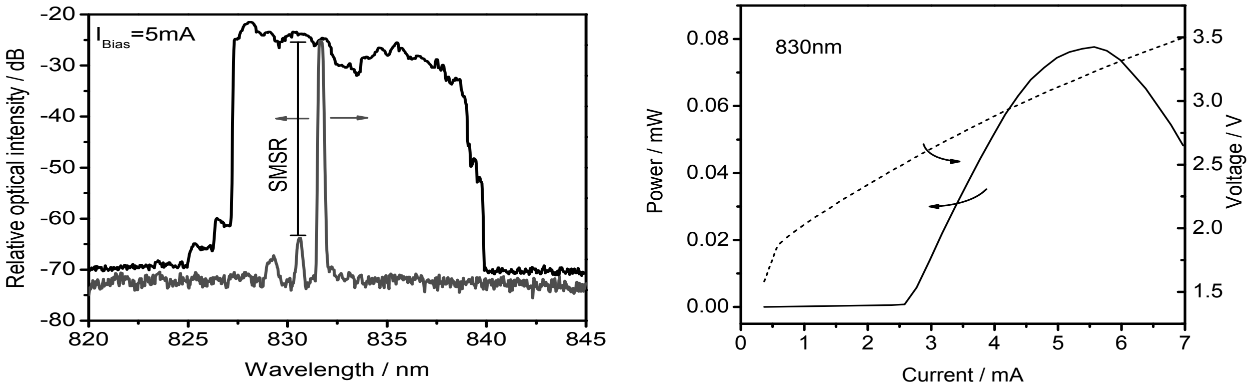

(a) (b)

Figure 6. (a) Fiber coupled spectrum of a device without the sub-wavelength grating. The envelope indicates the tuning range. (b) PIV-characteristic of the device at 830 nm.

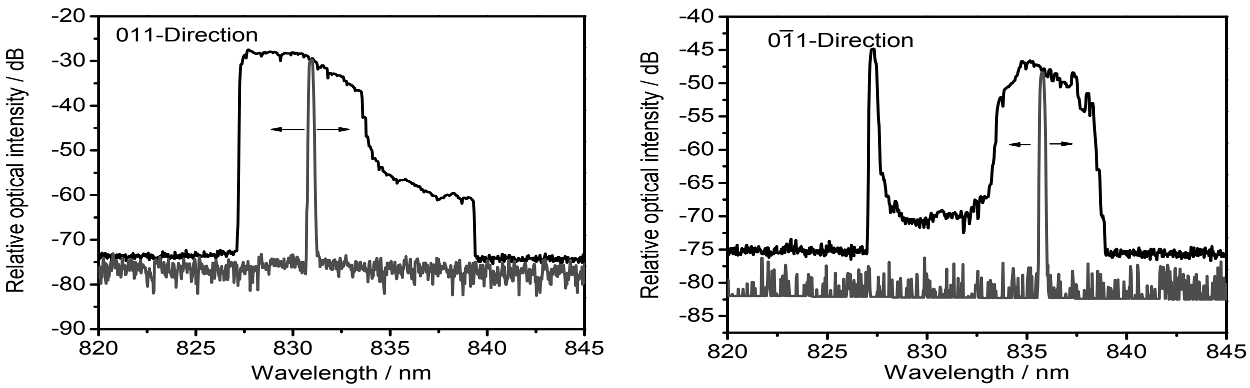

(a) (b)

Figure 7. Spectrum of the device without sub-wavelength grating after separating the polarization modes using the polarization setup (Fig. 5). (a) (011)-direction. (b) (0$\bar{1}$1)-direction.

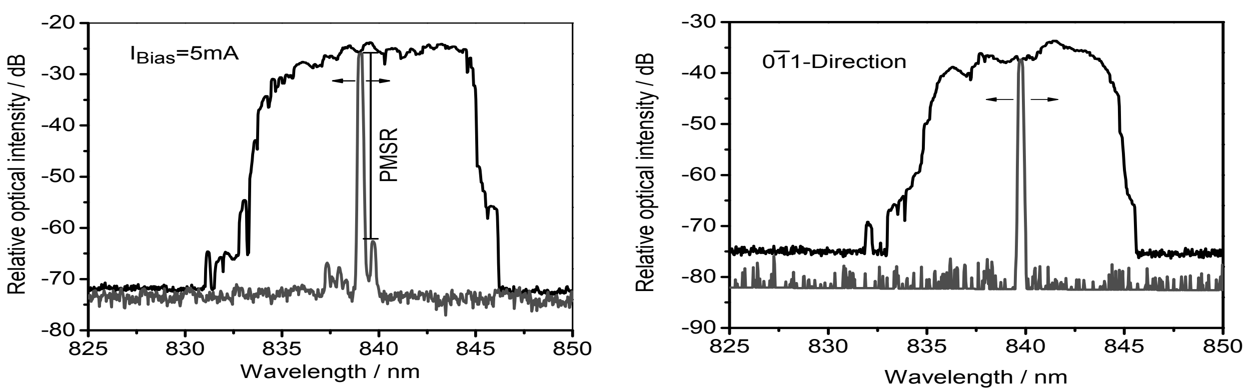

(a) (b)

Figure 8. (a) Fiber coupled spectrum of the VCSEL with sub-wavelength grating. (b) Spectrum of the device after separating the polarization modes using polarization setup (Fig. 5). The figure shows that the lasing mode over the entire tuning range is polarized in (0$\bar{1}$1)-direction.

dB has been measured during the tuning. By separating the polarization directions via using the setup shown in Fig. 5, it can be see that the dominant polarization which has been stabilized by sub-wavelength grating is the one in (0$\bar{1}$1)-direction which remains stable during the tuning and does not switch to the (011)-direction (Fig.

8b). The state of polarization remains stable for different laser bias currents too. For two wavelength of 839 nm and 843 nm the IV-characteristic are shown in Fig. 9. There can be seen that the polarization mode polarized in $(0\bar{1}1)$-direction remains the dominant one even for different laser bias currents.

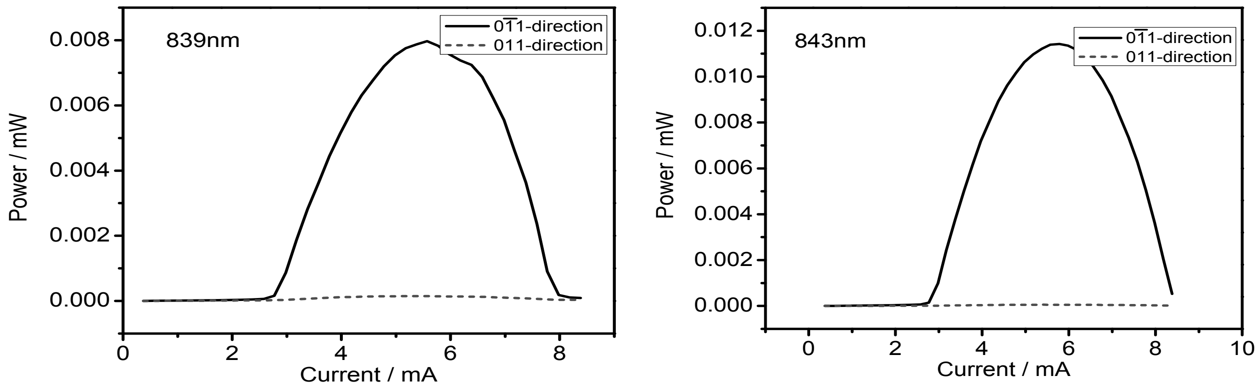

(a) (b)

Figure 9. PI-characteristic of both polarization direction using the polarization setup (Fig. 5). (a) At a wavelength of 839 nm. (b) at a wavelength of 843 nm.

4. CONCLUSION

In conclusion we presented a single-mode tunable VCSEL with a stable state of polarization. The single-mode operation has been achieved by adjusting the beam waist of the fundamental mode into the oxide aperture. With this method a SMSR of larger than 30 dB has been achieved. To stabilize the state of polarization a sub-wavelength grating has been implemented on top of the half-VCSEL. The introduced sub-wavelength grating is implemented in (011)-crystallographic direction and stabilizes the polarization in perpendicular direction. A PMSR of more than 35 dB has been achieved for the device during tuning. The device shows a stable SOP for different laser bias currents too.

ACKNOWLEDGMENTS

The content of this work is based on the work which has been performed in the European FP7 STREP project "SUBTUNE" under the Grant agreement number 224572.

REFERENCES

1. R. R. Patel, S. W. Bond, M. D. Pocha, H.E. Garrett, R. F. Drayton, H. E. Peterson, D. M. Krol, R. J. Deri, M. E. Lowry. "Multiwavelength parallel optical interconnects for massively parallel processing" in *Selected topics in quantum electronics*,Vol. 9, Issue 2, pp.657-66, 2003.
2. I. Artundo, L. Desmet, W. Heirman, C. Debaes, J. Dambre, J.M. Van Campenhout, H. Thienpont. "Selective optical broadcast component for reconfigurable multiprocessor interconnects" in *Selected topics in quantum electronics*,Vol. 12, Issue 4. pp.828-837, 2006.
3. Å. Haglund, J. S. Gustavsson, Jö. Bengtsson, P. Jedrasik and A. Larsson. "Design and evaluation of fundamental-mode and polarization-stabilized VCSELs with a subwavelength surface grating" in *IEEE journal of quantum electronics*,Vol. 42, No. 3. pp.231-240, 2006.
4. J. M. Ostermann, P. Debernardi and R. Michalzik"Surface-grating VCSELs with dynamically stable light output polarization" in *IEEE photonics technology letters*,Vol. 17, No. 12. pp.2505-2507, 2005.
5. J. S. Gustavsson, Å. Haglund, E. Söderberg S, J. Vukusic, P. Modh, P. Jedrasik and A. Larsson. "Mode and polarization control in VCSELs using shallow surface structures" in *Optoelectrinics, IET*,Vol. 1, No. 5. pp.197-205, 2007.

6. H. A. Davani, C. Grasse, B. Kögel, P. Westbergh, C. Gierl, K. Zogal, S. Jatta, G. Böhm, T. Gründl, P. Meissner, A. Larsson and M-C. Amann. "Widely tunable high-speed bulk-micromachined short-wavelength MEMS-VCSEL" *IEEE Semiconductor Laser Conference 2010,ISLC*, pp. 9-10, 2010.
7. M. Takahashi, N. Egami, T. Mukaihara, F. Koyama and K. Iga."Lasing characteristics of GaAs(311)A substrate based In GaAs-GaAs vertical-cavity surface-emitting lasers" in *IEEE J. sel. top. Quantum Electron.* ,Vol. 3, pp.372-378, 1997.
8. N. Nishiyama, M. Arai, S. Shinada, M. Azushi, T. Miyamoto, F. Koyama and K. Iga. "Highly strained GaInAs-GaAs quantum-well vertical-cavity surface-emitting laser on GaAs (311)B substrate for stable polarization operation" in *IEEE J. sel. top. Quantum Electron.* ,Vol. 7, pp.242-248, 2001.
9. G. Verschaffelt, W. van der Vleuten, M. Creusen, E. Smalbrugge, T.G. van de Roer, F. Karouta, R.C. Strijbos, J. Veretennicoff, B. Ryvkin, H. Thienpont and G. A. Acket. "Polarization stabilization in vertical-cavity surface-emitting lasers through asymetric current injection" in *IEEE Photon. Technol. Lett.*,Vol. 12, pp.945-947, 2000.
10. L.J. Sargent, J.M. Rorison, M. Kuball, R.V. Penty, I.H. White, S.W. Corzine, M.R.T. Tan, S.Y. Wang and P.J. Heard "Investigation of polarization pinning mechanism in deep-line-etched vertical-cavity surface-emitting lasers" in *Appl. Phys. Lett.*,Vol. 76, pp. 400-402, 2000.
11. F. Monti di Sopra, M. Brunner and R. Hovel "Polarization control in strained T-bar VCSELs" in *IEEE Photon. Technol. Lett.*,Vol. 14, pp. 1034-1036, 2002.
12. F. Sugihwo, M.C. Larsson and J.S. Harris"Micromachined widely tuneable vertical cavity laser diodes" in *Journal of Microelectromech. Syst.*,Vol. 7, No. 1 pp. 48-55, 1998.
13. F. Riemenschneider, I. Sagnes, G. Böhm, H. Halbritter, M. Maute, C. Symonds, M.-C. Amann and P. Meissner "A new concept for tunable long wavelength VCSELs," *Optics Communications.,*vol. 222, pp. 341-350, July 2003.
14. J. S. Gustavsson, Å. Haglund, J. Vukusic, J. Bengtsson, P. Jedrasik and A. Larsson. "Efficient and individually controllable mechanisms for mode and polarization selection in VCSELs, based on a common, localiezed, sub-wavelength surface grating" in *Opt. Express*,Vol. 13, No. 17. August, 2005.
15. P. Debernardi, and G. P. Bava. "Coupled mode theory: a powerful tool for analyzing complex VCSELs and designing advances features" in *IEEE J. selected topics Quantum electron., optoelectronic devices simulation*,Vol. 9, No. 3., pp. 905-917, 2003.